

Studying ΛN interactions through the $^{208}\text{Pb}(e,e'K^+)^{208}\Lambda\text{Tl}$ reaction

Franco Garibaldi^{1,*}, Omar Benhar¹, Petr Bydovsky², Toshiyuki Gogami³, Silviu Covrig⁴, Pete E.C. Markowitz⁵, John Millener⁶, Toshio Motoba⁷, Sho Nagao⁸, Satoshi N. Nakamura^{8,9}, Joerg Reinhold⁵, Liguang Tang^{4,10}, Guido Maria Urciuoli¹, and Isaac Vidana¹¹

¹Istituto Nazionale di Fisica Nucleare, Sezione di Roma, P. A. Moro Rome, Italy

²Nuclear Physics Institute, 250 68 Rez, Czech Republic

³Department of Physics, Graduate School of Science, Kyoto University, Kyoto, Kyoto 606-8502 Japan

⁴Thomas Jefferson National Accelerator Facility, Newport News, Virginia 23606, USA

⁵Florida International University, Miami, Florida 33199, USA

⁶Brookhaven National Laboratory, Upton, New York 11973, USA

⁷Osaka University, Japan

⁸Department of Physics, Graduate School of Science, Tohoku University, Sendai, Miyagi 980-8578, Japan

⁹Department of Physics, Graduate School of Science, The University of Tokyo, Hongo, Tokyo 113-0033, Japan

¹⁰Department of Physics, Hampton University, Hampton, Virginia, 23668, USA

¹¹Istituto Nazionale di Fisica Nucleare, Sezione di Catania, Catania, Italy

Abstract. The hyperon puzzle, the observation that the two-solar-mass neutron star existence is hardly explained by all models predicting the appearance of hyperons in the neutron star core, is currently one of the unsolved key issues in the physics of compact stars. To solve the hyperon puzzle an experimental program has been proposed by the Jefferson lab hypernuclear collaboration and approved by the Jefferson Lab (JLab) PAC. This program consists in the study of the reaction $(e, e'K)$ on ^{40}Ca and ^{48}Ca nuclei, aimed at investigating the isospin dependence of hyperon dynamics, and in the study of the reaction $(e, e'K)$ on ^{208}Pb nucleus, which is the subject of this paper and which will take advantage of the fact that ^{208}Pb properties largely reflects those of the uniform nuclear matter present in the interior of the neutron stars making it the ideal tool to investigate neutron star features. The proposal of the study of the reaction $(e, e'K)$ on ^{208}Pb was approved by the Jlab PAC in 2020.

1 Introduction

An ambitious and challenging experimental program, aimed at obtaining high-resolution hypernuclear spectroscopy via the $(e, e'K^+)$ reaction, was started at Jefferson Lab almost 20 years ago. The data, taken in both Hall A and Hall C using p-shell and medium-mass nuclear targets, have provided clear spectra with $\sim 0.5\text{--}0.8\text{-MeV}$ energy resolution [1,2]. The process, whose feasibility has been established at JLab, is now widely recognized as a powerful tool to study hypernuclear spectroscopy, in addition to the (K, π) and (π^+, K^+) reactions. Electron- and hadron-induced reactions are in fact complementary to one another, being predominantly driven by spin-flip and non-spin-flip mechanisms, respectively. Furthermore, the $(e, e'K^+)$ reaction allows for a much better energy resolution and produces mirror hypernuclei with respect to those produced with hadron probes.

The JLab hypernuclear collaboration proposed to the Jefferson Lab PAC43 a coherent series of studies of the $(e, e'K^+)$ reaction, to be performed using targets spanning a wide range of mass. The purpose of this analysis was the investigation of the ΛN interactions in a variety of nuclear media. The PAC43 identified the study of the isospin dependence as the highest priority, and conditionally approved the $^{40}\Lambda\text{K}$ and $^{48}\Lambda\text{K}$ binding energy measurements. The JLab hypernuclear collaboration re-submitted to PAC 2016 the proposal which was approved.

The recent observation of two-solar-mass neutron stars, whose existence cannot be explained by all models predicting the appearance of hyperons in the neutron star core and which is known as “hyperon puzzle”, strongly suggests that our understanding of nuclear interactions involving hyperons is not adequate for a fully quantitative description of neutron star matter. Unfortunately, the information provided by the available scattering data in the hyperon-nucleon (YN) sector is scarce, and does not allow the determination of the YN potential using the same scheme successfully employed in the nucleon-nucleon (NN) sector. Presently, hypernuclear spectroscopy appears to be the only practical way to study baryonic forces, and may play a significant role towards the solution of the hyperon puzzle.

In view of its important astrophysical implications, the extension of the $(e, e'K^+)$ experimental program to a heavy nuclear target with large neutron excess, such as ^{208}Pb , is of primary importance. The study of the $^{208}\text{Pb}(e, e'K^+)^{208}\Lambda\text{Tl}$ reaction which would provide information on the properties of a bound hyperon in an environment little affected by

*Corresponding author: franco.garibaldi7@gmail.com

surface and shell effects is complementary to the measurements on ^{40}Ca and ^{48}Ca targets, whose main purpose is the analysis of the isospin dependence of hyperon dynamics.

The measured charge density distribution of ^{208}Pb [3] clearly shows (see Fig. 1b) that the region of nearly constant density accounts for a very large fraction ($\sim 70\%$) of the nuclear volume, thus suggesting that its properties largely reflect those of uniform nuclear matter in the nuclear star interior (see Fig. 1a). The validity of this conjecture has been long established by a comparison between the results of theoretical calculations and the data extracted from the $^{208}\text{Pb}(e,e'p)^{207}\text{Tl}$ cross sections measured at NIKHEF in the 1980s [4,5] (Fig. 1a).

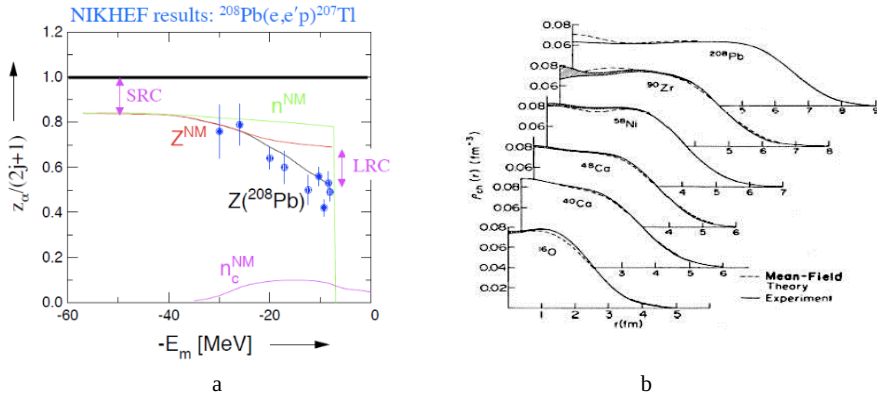


Fig. 1a. Energy dependence of the spectroscopic factors (occupation probabilities n and hole-state strengths Z) extracted from the measured $^{208}\text{Pb}(e,e'p)^{207}\text{Tl}$ cross sections [4,5], compared to the theoretical results of Ref. [6]. The black and red solid lines, labelled $Z^{(208\text{Pb})}$ and Z^{NM} , correspond to ^{208}Pb and uniform nuclear matter, respectively. The effects of short- (SRC) and long-range-correlations (LRC), the latter arising from surface and shell effects, are indicated.
Fig. 1b. charge density distribution of ^{208}Pb compared to lighter nuclei.

As shown in Fig.1 the energy dependence of the spectroscopic factors, obtained from the analysis of the measured missing energy spectra, turns out to be in remarkably good agreement with the results reported in the pioneering work of Ref. [6]. Short-range correlations appear to be the most important mechanism leading to the observed quenching of the spectroscopic factor, while surface and shell effects only play an important role in the vicinity of the Fermi surface. The picture emerging from Fig. 1 suggests that deeply bound protons in the ^{208}Pb ground state behave as if they were in nuclear matter. Figure 2, provides a schematic representation of the $(e,e'K^+)$ reaction, illustrating the connection with the corresponding $(e,e'p)$ process. The left and right boxes highlight the amplitudes determined by nuclear and hypernuclear dynamics, described by the nucleon and hyperon spectral functions, respectively.

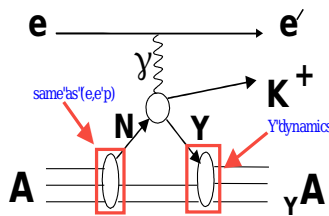


Fig. 2. Schematic representation of the $(e,e'K^+)$ reaction. The left and right boxes highlight the amplitudes involved in the proton and Λ spectral functions, respectively.

The availability of the information obtained from the measured $(e,e'p)$ cross sections is critical for the interpretation of $(e,e'K^+)$ data. To see this, just consider that the hyperon binding energies are given by the difference between the missing energy measured in $(e,e'K^+)$ and the proton binding energies obtained from $(e,e'p)$ cross section. Hence, $(e,e'p)$ data will provide the baseline needed to extract information on hyperon binding energies.

The results of theoretical calculations of the hyperon spectral function and the wealth of available $^{208}\text{Pb}(e,e'p)$ data, including binding energies and widths of the many proton states, will allow us to develop a fully realistic model of the $^{208}\text{Pb}(e,e'K^+)$ cross section, indispensable for the extraction of the information on hypernuclear dynamics.

2 Spectroscopic study of $^{208}_{\Lambda}\text{Tl}$ trough the $^{208}\text{Pb}(e,e'K^+)^{208}_{\Lambda}\text{Tl}$ reaction

So far, the spectroscopy of heavy hypernuclei has been studied with pion and kaon beams which do not allow for adequate accuracy and precision. The main issue was the poor resolution, 1.6 MeV (FWHM). In addition, the spacing

between Λ single-particle states is only 4 to 6 MeV. As a result, the existing data do not resolve the two series of states, introducing uncertainties in the theoretical analyses. The absolute binding energies of all (π^+ , K^+) hypernuclear data are based on the 6 events of $^{12}\Lambda\text{C}$ emulsion data, while in the case of ($e, e'K^+$) experiments the absolute energy scale can be calibrated exploiting the elementary $p(e, e'K^+)\Lambda/\Sigma^0$ processes. The recent and precise hypernuclear data on $^{12}\Lambda\text{B}$ and $^{16}\Lambda\text{N}$ collected at JLab, combined with a careful re-examination of the consistency between emulsion data, point to a possible half-MeV shift of the $^{12}\Lambda\text{C}$ ground state energy, which would greatly impact on every hypernuclear binding energy measured using the reaction (π^+ , K^+). Precise hypernuclear spectroscopy on medium to heavy hypernuclei with electron beams, which is only possible with the CEBAF electron beam, is critically important to obtain new information needed to constrain theoretical models of neutron star matter.

The ($e, e'K^+$) reaction enables the determination of binding energies with high precision because of the calibration provided by the elementary reaction on hydrogen and is currently the only method that can measure the absolute centroids of peak doublets, which naturally emerge in hypernuclear missing mass spectroscopy, with an unprecedented accuracy of <100 keV. It provides information on the cross section as well as on the binding energy.

Microscopic calculations of the Λ spectral function in a variety of nuclei, ranging from ^5He to ^{208}Pb , have been recently carried out [7]. The results of this analysis, based on a realistic hyperon-nucleon potential model constrained by the available scattering data, suggest that hyperon dynamics in ^{208}Pb may be somewhat different compared to lighter nuclei, as shown by a larger quenching of the spectroscopic factors.

The study of ^{208}Pb with the ($e, e'K^+$) reaction will provide a better binding energy resolution than that of the experiments performed so far with hadronic probes and thus a more detailed understanding of baryon behaviour deep inside of the nucleus, providing important information for studying the Λ single-particle nature under high nucleon density. ^{208}Pb is the ideal target to study hyperons in a medium closely resembling neutron star matter. This environment is best suited to investigate the effects of three body forces involving hyperons [8-11] which increase the stiffness of the nuclear matter equation of state, thus allowing for the existence of massive neutron stars compatible with the observational constraints.

In conclusion, even if the typical baryon density inside a neutron star is much higher than in a hypernucleus a precise knowledge of the ^{208}Pb level structure can, by constraining the hyperon-nucleon potential, contribute to more reliable predictions regarding the internal structure of neutron stars, and in particular their maximum mass.

3 The proposed experiment

The aim of the experiment is measuring the $^{208}\text{Pb}(e, e'K^+)\Lambda^{208}\text{Tl}$ reaction. Fig. 3a shows the missing mass spectrum obtained by the $^{208}\text{Pb}(\pi^+, K^+)\Lambda^{208}\text{Pb}$ reaction [12]. It shows a characteristic bump structure starting from the binding energies B_Λ around 25 MeV.

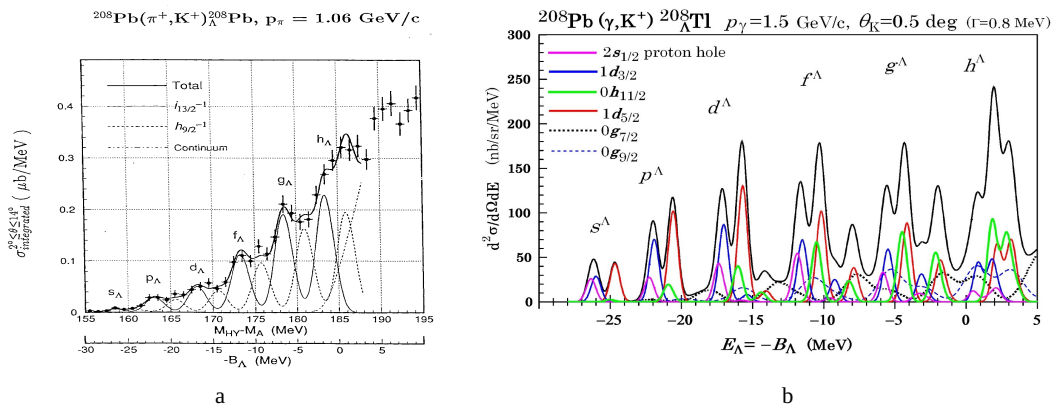


Fig. 3a. Binding energy spectrum of $^{208}\Lambda\text{Pb}$ measured in E140 experiment. **Fig. 3b.** ^{207}Tl core nucleus level scheme (Motoba-Millener calculation)

The experiment will make it possible to determine with much better precision the binding energies thanks to the calibration achievable exploiting the elementary $p(e, e'K^+)\Lambda/\Sigma^0$ processes with hydrogen [1] and to test both the dynamical models and the computational techniques employed in the available theoretical approaches.

Spectroscopic data exist for few Λ hypernuclei obtained through the ($e, e'K^+$) reaction and few others would be available on ^{40}Ca and ^{48}Ca . Consequently it is extremely important to perform ($e, e'K^+$) experiment also on ^{208}Pb . The much better energy resolution of binding energy spectra of hypernuclei generated through the ($e, e'K^+$), a factor of ~ 3 better than in spectra of hypernuclei generated with π^+ or K^- as probes (see Fig. 3a and 3b), will make it possible the determination of much more precise Λ single-particle energies. It will be possible to “see” deep shells, in practice not

visible with (π, K) reaction (“the observed small peaks *are assumed to be the s_Λ states*” [12]). Fig. 3b shows the Excitation Energy Spectrum for the $^{208}\text{Pb}(e, e'K^+)^{208}\Lambda\text{Tl}$ reaction, calculated by Millener and Motoba for the kinematics originally planned for the experiment in the Hall A of JLab [13] using the Saclay-Lyon elementary (SLA) amplitude [14]. The Λ is assumed to be weakly coupled to the proton-hole states of ^{207}Tl strongly populated in ($e, e'p$) or ($d, ^3\text{He}$) reactions on ^{208}Pb [15]. The Λ single-particle energies were calculated from a Woods-Saxon well fitted to energies derived from the $^{208}\text{Pb}(\pi^+, K^+)^{208}\Lambda\text{Pb}$ reaction. Just a few states cannot be resolved: states based on the closely-spaced $p\ 2s_{1/2}^{-1}$ and $p\ 1d_{3/2}^{-1}$ states, (blue bars and curves), the $p\ 0h_{11/2}^{-1}$ and $p\ 1d_{5/2}^{-1}$ states (red bars and curves). The successive red and blue peaks correspond to the population of the $0s, 0p, 0d, 0f, 0g,$ and $0h$ Λ orbits. The green lines correspond to the noded $1s, 1p, 1d/2s,$ and $1f$ Λ orbits. The remaining (wiggly) curves correspond to strength based on deeper and fragmented proton-hole strength. Once the Λ single-particle energies are known for Pb, many-body calculations using the Auxiliary Field Diffusion Monte Carlo (AFDMC) approach [8] can be used to try to determine the balance between the spin-independent components of the ΛN and ΛNN interactions required to fit Λ single-particle energies across the entire periodic table. The Λ binding energy extracted will provide most valuable information, needed to constrain the models of hyperon interaction in nuclear matter.

4 The target

A major concern in the design of the experiment was developing a Pb target that could operate at high beam currents without melting. We considered the setup used at NIKHEF for ($e, e'p$) experiment [5]. This would allow us to run safely with $10\ \mu\text{A}$ of beam current and $100\ \text{mg}/\text{cm}^2$ of pure ^{208}Pb target. However, using the same setup but cooling with a cryogenic we will be allowed to use higher beam currents ($25\ \mu\text{A}$) in order to increase the counting rate and hence to improve the “detectability” of the small peaks. Fig 4 shows that we would be able to run safely with a beam current of $25\ \mu\text{A}$ provided that a raster area not smaller than $2 \times 2\ \text{mm}^2$ is used [16]. The results were obtained with Computational Fluid Dynamics simulations, assuming that the Pb foil would be held in the target frame used in the experiment PREX-II.

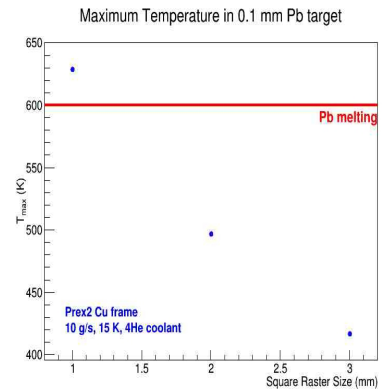


Fig. 4. Maximum temperature of the Pb target as function of the raster area for a beam current of $25\ \mu\text{A}$.

5 Particle identification

The identification of kaons detected in the hadron arm against a huge background of protons and pions is one of the major challenge of the experiment. To reduce the background level in produced spectra, a very efficient PID system is necessary for unambiguous kaon identification. In the electron arm, the gas Čerenkov counters [17] give pion rejection ratios up to 10^3 . The dominant background (knock-on electrons) is reduced by 2 further orders of magnitude by the lead glass shower counters, giving a total pion rejection ratio of 10^5 [18]. The lead-glass shower counters and the gas Čerenkov are calibrated against each other.

The PID system in the hadron arm (HKS) is composed of: three planes of time-of-flight counters, two planes of water Čerenkov counters, and three planes of aerogel Čerenkov counters (see Fig. 5a). The power rejection capability of the HKS hadron identifier is 4.7×10^{-4} [19] (see Fig. 5b).

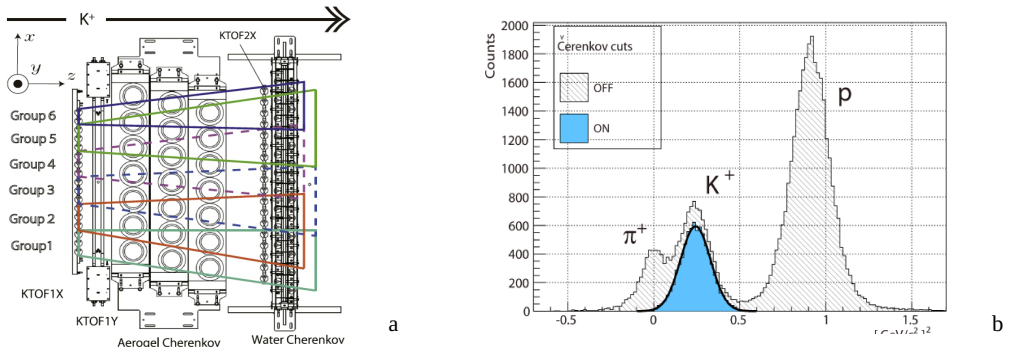


Fig. 5a. HKS PID (see text); **Fig. 5b.** HKS kaon power identification

Combining the HKS hadron identification detectors with the RICH would allow us to obtain the almost unprecedented separation power of 10^{12} [21].

Fig. 6 shows the performance of the Hall A RICH detector [20,21].

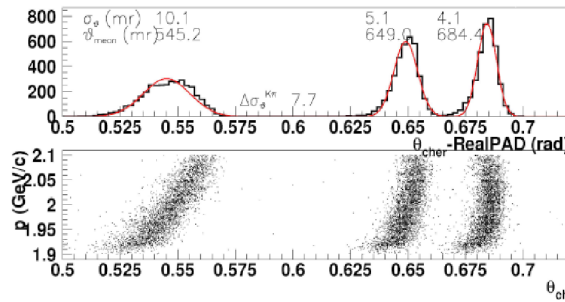


Fig. 6. Upgraded RICH simulated performance: Pion/Kaon Čerenkov angle distribution, with equal hadrons populations, at 2 GeV/c momentum, in the HRS spectrometer acceptance. The Montecarlo is tuned on Hall A hypernuclear experimental data.

6 Kinematics and counting rate

The experiment has been approved by the Jlab PAC to run in Hall A using the spectrometer HRS_L to detect scattered electrons and the spectrometer HKS to detect kaons. Nevertheless, due to unavailability of the Hall A for this experiment in the next 10 years we will be obliged to run in Hall C using the spectrometer HES to detect electrons and the spectrometer HKS to detect kaons. In Fig. 7 we show the new experimental setup. The new kinematics of the experiment is: $E_{\text{beam}} = 2.34 \text{ GeV}$, $\Theta_{e^e} = 8^\circ$, $p_e = 0.84 \text{ GeV/c}$, $\Theta_{e\gamma} = 4.5^\circ$, $E_\gamma = 1.5 \text{ GeV}$, $\Theta_{K\gamma} = 8^\circ$, $p_K = 1.2 \text{ GeV/c}$.

The counting rates, calculated in the new experimental setup in Hall C, at a current of 25 μA , an energy resolution of 800 keV and a target thickness of 100 mg/cm^2 , are shown in Table 1. The counting rates and the Signal to Noise Ratio (SNR) were calculated by Montecarlo simulations as well as a comparison with the K^+ background detected during experiment E05-115 which used the same apparatus setup but a new pair of charge separation dipole magnets (PCS) instead of the splitter. The SNR refers to cross section calculations of the $^{208}\text{Pb}(e,e^+K^+)^{208}\text{Atl}$ reaction only at a very preliminary stage.

Table 1. Counting rates

Target	Beam current (μA)	Target thickness (mg/cm^2)	Assumed cross section (nb/sr)	Expected yield (/hour)	Number of events	Requested Beam time (hours)	B.G. Rate (MeV/h)	S/N
^{208}Pb	25	100	80 (g.s.)	0.24	115	480	0.084	18.5

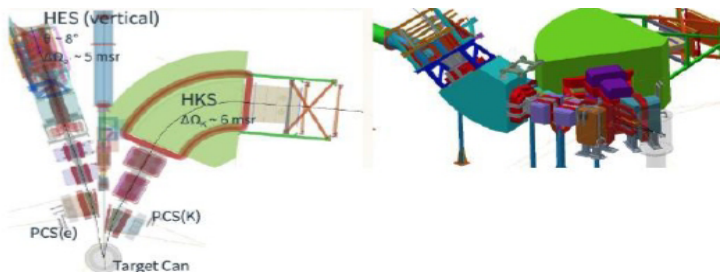


Fig. 7. The experimental setup in Hall C.

7 Summary and conclusions

The experiment on ^{208}Pb described in this paper is an essential part of the campaign of measurements the Jefferson Lab hypernuclear collaboration is doing. It allows us to extend the A (mass number) range of the hypernuclear binding energy spectroscopy to its extreme. The mass number dependence of the binding energy for each shell model orbital will be extended to $A = 208$. The study of the $^{208}\text{Pb}(e,e'K^+)^{208}_{\Lambda}\text{Tl}$ reaction together with the other reactions proposed to Jefferson Lab PAC by the same collaboration will “complete” the systematic study of Λ hypernuclear bound states over a wide mass range. It will also deepen our understanding of the nature of the ΛN and ΛNN interactions in nuclear medium. Moreover, together with the spectroscopy studies already performed at JLab, and proposed to the JLab PAC (the approved experiment on ^{40}C and ^{48}Ca) may play a significant role towards the solution of the so-called hyperon puzzle.

8 References

1. F. Garibaldi et al., Phys. Rev. C **99**, 054309 (2019); arXiv:1807.09720
2. S.N. Nakamura, T. Gogami and L. Tang, JPS Conf. Proc., 011002 (2017)
3. B. Frois and C. N. Papanicolas, Ann. Rev. Nucl. Part. Sci. **37**, 133 (1987)
4. E. N. Quint et al., Phys. Rev. Lett. **56**, 186 (1986); E. N. Quint et al., *ibid.* **58**, 1727 (1987)
5. M. van Batenburg, PhD Thesis, University of Utrecht, 1996
6. O. Benhar, A. Fabrocini, and S. Fantoni, Phys. Rev. C **41**, R24 (1990)
7. I. Vidaña, Nucl. Phys. **958**, 468 (2017)
8. D. Lonardoni, F. Pederiva, and S. Gandolfi, Phys. Rev. C **89**, 014314 (2014)
9. D. Lonardoni, A. Lovato, S. Gandolfi, and F. Pederiva, Phys. Rev. Lett. **114**, 092301 (2015)
10. B. Sharma, Q.N. Usmani and A.R. Bodmer, arXiv:110 2.1542
11. Bobeldij et al. Phys. Rev. **73**, 2684 (1994)
12. O. Hashimoto and H. Tamura, Progress in Particle and Nuclear Physics **57**, 564 (2006)
13. J. Millener, personal communication
14. C. David, C. Fayard, G.-H. Lamot, B. Saghai, Phys. Rev. C **53**, 2613 (1996); T. Mizutani, C. Fayard, G.-H. Lamot, B. Saghai, Phys. Rev. C **58**, 75 (1998)
15. M. Sotona, personal communication
16. S. Covrig, personal communication
17. M. Iodice et al., Nucl. Instrum Methods Phys. Res. A **411**, 223 (1998)
18. J. Alcorn et al., Nucl. Instrum. Methods Phys. Res. A **522**, 294 (2004)
19. T. Gogami et al, Nucl. Instrum Methods A **900**, 69 (2018)
20. F. Garibaldi et al., Nucl. Instrum. Methods Phys. Res. A **502**, 117 (2003)
21. E Cisbani, personal communication